On the Rate Monitoring Performance of Active Learning-based Classifier for PCS-based Rate-flexible TWDM-CPON

Zixian Wei, Jinsong Zhang, Weijia Li and David V. Plant
Department of Electrical and Computer Engineering, McGill University, Montreal, QC H3A 0E9, Canada
E-mail address: zixian.wei2@mail.mcgill.ca, jinsong.zhang@mail.mcgill.ca

Abstract: We firstly demonstrated an active learning (AL)-based classifier for monitoring the entropy/rate of the PCS-based rate-flexible TWDM-CPON. For an 80-km 350-Gb/s/λ~450-Gb/s/λ downstream, AL-based scheme achieves 100%/95% entropy/rate identification accuracies corresponding to 25/5 Gbps tuning steps. © 2022 The Author(s)

1. Introduction

With the explosive growth of the information scale of Internet applications such as cloud computing, big data-based artificial intelligence (AI), and augmented reality/virtual reality (AR/VR) streaming media, the previous access network facilities have urgently needed upgrading to meet the requirements of ultra-high-speed and rate-flexible passive optical network (PON) [1]. On the one hand, with the increase in rate and performance requirements, the number of access optical network units (ONUs) also increases over a ~80-km metro access ring from an optical line terminal (OLT) [2]. The development of simplified coherent detection technology reduces the cost and promotes the development of coherent optical communication to medium and short distances. Coherent access such as >100-G time-wavelength division multiplexing (TWDM) coherent PON (CPON) is considered as next-generation mainstream PON architecture [3, 4].

On the other hand, more adaptive and flexible rate changes must be developed to accommodate different channels and access points. Previous subcarrier division scheme in the frequency domain has achieved remarkable results in rate adaptation [5]. While probabilistic constellation shaping-based (PCS-based) with tunable spectral efficiency (SE) characteristics enable a more continuous rate-adaptative scheme by varying the entropy of the transmitted signal [6-8]. Thus, combining PCS with variable entropy and TWDM-CPON can not only improve capacity and performance but also flexibly allocate spectrum for large-scale access users. Regulating rate through time-varying entropy requires an entropy/rate monitoring scheme at the receiver. However, there is no mechanism and discussion to monitor the changing rate/entropy in PCS-based optical systems or networks.

In this work, a rate-flexible TWDM-CPON setup is presented with a 350-Gb/s/λ ~ 450-Gb/s/λ for a specific ONU group. The minimum rate tunable rate step is single-polarized 5 Gbps at 50 Gbaud, corresponding to an entropy step of 0.1. For monitoring the entropy/rate varies in the TWDM-CPON, for the first time, an active learning (AL)-based image classifier is proposed, designed, and verified at the post-digital signal processing (DSP) of the coherent receiver after 80-km transmission. In addition, to illustrate the trade-off between classification accuracy and complexity, we compared different image classifiers based on different working principles.

2. Principles, Architecture and Experimental Setup

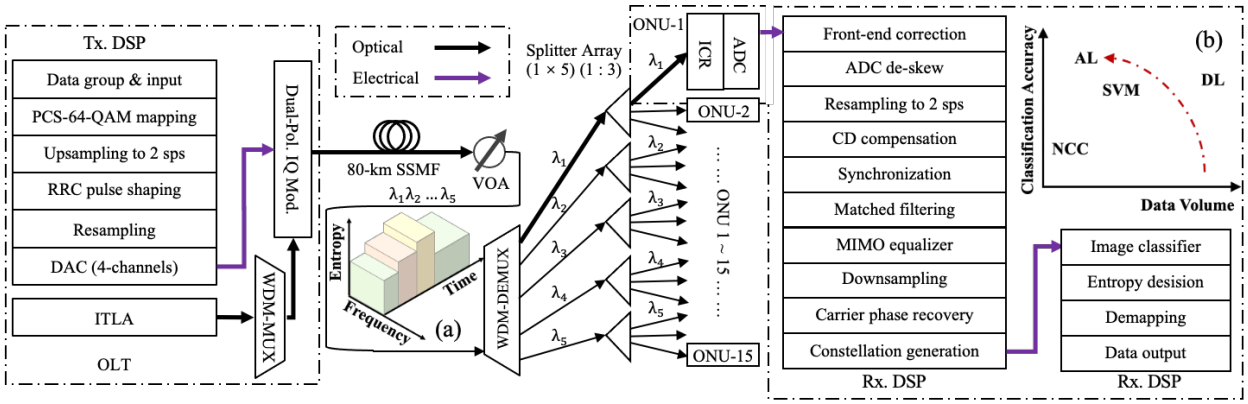

Fig. 1. The 350-Gb/s/λ ~450-Gb/s/λ downstream experimental setup for PCS-based rate-flexible TWDM-CPON with image classifier-based entropy/rate monitoring. Inset figures: (a) The frame structure of flexible rate by time-variant entropy for different ONUs; (b) General performance comparisons between training data volume and classification accuracy with classifiers based on different principles in our work.

Figure 1 illustrates the schematic of the proposed entropy-regulated rate-flexible TWDM-CPON architecture and downstream experimental setup. At the transmitter (Tx.), the rate-flexible signal is generated by tuning the entropy value at different continuous time slots. The specific digital signal processing (DSP) for 4-channel dual-polarized IQ signals include PCS-64-QAM mapping, upsampling to 2 sps, RRC pulse shaping, resampling, and digital-to-analog converter (DAC), respectively. The electrical signal and the carrier lightwave from micro-integrable tunable laser assembly (micro-ITLA) overlapped inside a dual-polarized IQ modulator (DP-IQ Mod.), and they passed through an 80-km standard single-mode fiber (SSMF). The receiving optical power level to different ONUs can be changed by a variable optical attenuator (VOA). The inset Figure 1(a) shows a time frame stream with various entropy-regulated rates, which is packaged and delivered to all the ONUs. At the receiver (Rx.), a micro-ICR and an ADC are set to receive the signal, while the demodulation DSP can be divided into a signal recovery part and an entropy identification part. The converted electrical signal is firstly front-end corrected. Then analog-to-digital converter (ADC) de-skew, resampling to 2 sps, chromatic dispersion (CD) compensation, synchronization, matched filter, multi-input multi-output (MIMO) equalization, downsampling, and carrier phase recovery are executed sequentially. Then, the classifier will determine whether the entropy/rate has changed between each time slot according to the point distribution of the acquired constellation, and further define the specific value of the entropy/rate.

The inset of Fig. 1(b) is a general performance comparison of image classifiers based on different principles, and the red dotted line is the designed optimized direction. The trade-off among computational complexity, recognition accuracy, and data overhead is the criteria leading to proposing AL-based classifiers. Generally, some deep learning (DL)-based classified schemes ask to collect large amounts of data to train networks and maintain accuracy. Machine learning (ML)-based schemes are a compromise, which can get better recognition and maintain a small data overhead. In addition, the methods based on numerical calculation require only a few data samples for reference, but the recognition accuracy is relatively low. Next, the proposed AL scheme is further compared with deep neural network (DNN), support vector machine (SVM), and simply normalized cross-correlation (NCC) calculation.

3. Results and Discussions

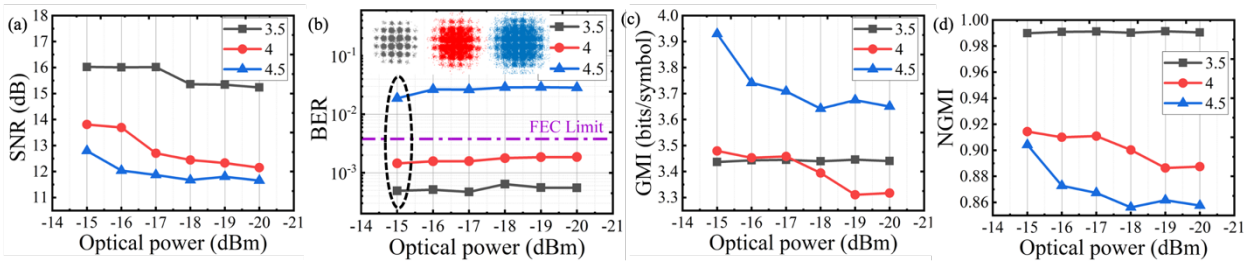

Fig. 2. System performances of single ONU with 1560 nm at 50.12 Gbaud: (a) SNR, (b) BER, (c) GMI, and (d) NGMI versus ROP from -15 dBm to -22 dBm with entropy varying from 3.5 to 4.5; (Inset figures in (b): the constellation diagrams at ROP of -15 dBm.)

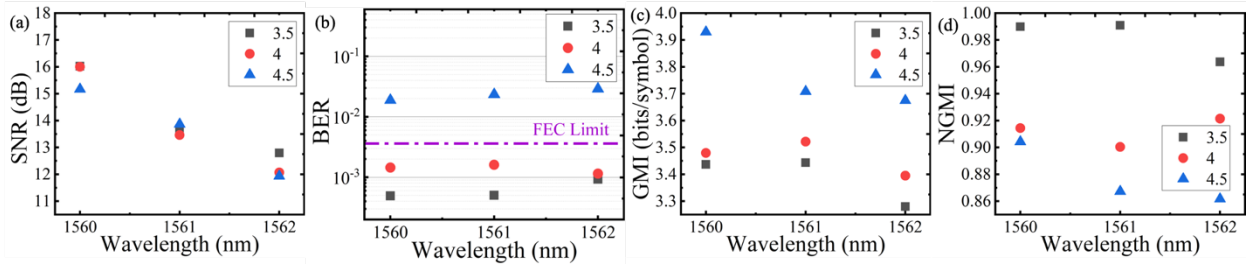

Fig. 3. System performances of multiple ONUs with the wavelength of 1560 nm, 1561 nm and 1562 nm at 50.12 Gbaud at -15 dBm ROP: (a) SNR, (b) BER, (c) GMI and (d) NGMI versus various wavelengths with entropy varying from 3.5 to 4.5.

In our TWDM-CPON setup, different ONUs groups are divided by wavelengths, while within the single ONUs group, the single ONU is divided by a 1:3 power splitter. Here, the entropy values are changed among 3.0, 4.0, and 4.5, corresponding to the rate changing from 350 Gb/s/λ ~ 450 Gb/s/λ with a minimum rate tuning step of 25 Gb/s/pol./λ. For the specific ONUs group at 1560 nm, as shown in Fig. 2, the communication performance has an obvious layering phenomenon with the changing of entropy. In Fig. 2(a), the SNRs decrease with the decreasing of the ROP, and at the ROP of -15 dBm, the SNR can reach 16.0238 dB with an entropy of 3.5. The diagram of BERs versus ROPs is further shown in Fig. 2(b). The transmitted signals with the entropies of 3.5 and 4.0 are capable of reaching the hard-decision forward error correction (HD-FEC) threshold of 3.8×10^{-3}, and the BER values are

4.9×10^{-4} and 1.45×10^{-3}, respectively. Inset figures in Fig. 2(b) are the PCS constellation diagrams of 3.5, 4.0, and 4.5 at -15 dBm, respectively. The constellation points spread out with increasing entropy. The corresponding generalized mutual information (GMI) and normalized generalized mutual information (NGMI) are further presented in Fig. 2(c) and Fig. 2(d). For example, at -15-dBm ROP and 1560 nm, the GMI and NGMI are 3.4368 and 0.9899 at the entropy of 3.5. A further experimental measurement is conducted to demonstrate the stability among different ONUs groups at -15 dBm. Three wavelengths of 1560 nm, 1561 nm, and 1562 nm are adopted to support three ONUs groups. From Fig. 3(a) and Fig. 3(b), although the SNRs slightly decrease from 1560 nm to 1562 nm, the BERs performance is fairly consistent and stable across carriers. Similarly, we show the measured GMI and NGMI at different entropies and carriers in Fig. 3(c) and Fig. 3(d).

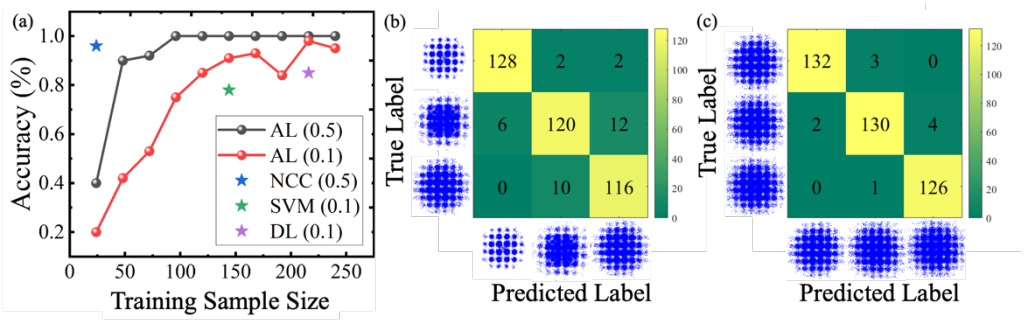

Fig. 4. Classification performances and comparisons: (a) Classification accuracies of various schemes verse different training sample volumes from 24 to 240 at an entropy interval of 0.5 (from 3.5 to 4.5) or 0.1 (from 4.5 to 4.7). (b) The confusion matrix of the AL-based scheme at the entropy of 0.5 and training sample size of 72 (Coordinates: 3.5, 4.0, 4.5; 92% identification accuracy). (c) The confusion matrix of the AL-based scheme at the entropy interval of 0.1 and training sample size of 216 (Coordinates: 4.5, 4.6, 4.7; 98% identification accuracy).

The overall identification performance is presented in Fig. 4. With few training samples, the AL-based scheme can achieve rapid convergence through the query mechanism in Fig. 4(a). At the entropy interval of 0.5 (black curve), corresponding to the entropies of 3.5, 4.0, and 4.5, the identification accuracy reaches 100% with only 96 training samples. Then, a confusion matrix with 92 % identification accuracy is further presented in Fig. 4(b) using 72 training samples. The abscissa constellation diagrams in Fig. 4(b) are with an entropy of 3.5, 4.0, and 4.5 with 0.5 intervals, respectively. When the step size of entropy/rate tuning is gradually reduced to 0.1/5 Gbps at 50 Gbaud, higher requirements are placed on the performance of the classifier. At 0.1 entropy interval, the AL-based classifier was able to improve the recognition accuracy of constellation maps to >91% under 144 training samples. Although there are some fluctuations in the curve with the increase in the sample size, it can be maintained above 90%. Next, Fig. 4(c) shows a confusion matrix with 98% identification accuracy with 216 training samples among 4.5, 4.6, and 4.7. In addition, in Fig. 4(a), NCC can reach a ~96% identification accuracy with 24 samples but only works when the entropy interval is large and rapidly ineffective as the entropy interval narrows from 0.5 to 0.1. For a finer rate tuning, SVM cannot reach a relatively high accuracy at a low training sample, while a DL-based classifier requires a large set of training samples with annotations.

4. Conclusions

To further increase the data rate and rate flexibility of next-generation PONs, we propose and demonstrate a 350-Gb/s/λ ~450-Gb/s/λ 80-km TWDM-CPON architecture with rate monitoring. The coherent PON is dynamically regulated with time-variant entropy and the transmitted frames allocated to different ONUs can be identified and distinguished by the value of entropy. A 0.5/0.1 interval value of entropy is precisely tuned to achieve a 100%/95% constellation identification accuracy by an AL-based image classifier, corresponding to rate tuning steps of 25 Gb/s and 5 Gb/s at 50 Gband. Due to the query mechanism, the AL-based entropy/rate identification scheme has shown advantages over other schemes in the case of a small sample size. Our work provides a powerful rate monitoring tool for the next-generation rate-adjustable optical access network.

This work was partly supported by the Fonds de recherche du Québec - Nature et technologies (FRQNT Grant No. 319934 and 319965). The authors also thank Ciena for use of a WaveLogic modem in their experiments.

References

[1] T. Pfeiffer, *et al.*, J. Opt. Comm. Netw., 14(1), A31-A40, (2022).
[2] LB. Du, et al., J. Lightwave Technol., 37(3), 688-697, (2018).
[3] MS. Faruk, *et al.*, IEEE Commun. Mag., 59(12), 112-117, (2021).
[4] G. Li, *et al.*, in OFC 2022, paper Th3E. 3.
[5] J. Zhang, *et al.*, in OFC 2020, paper W1E. 5.
[6] R. Zhang, *et al.*, in ECOC 2020, 1-4.
[7] R. Borkowski, *et al.*, J. Opt. Comm. Netw., 14(6), C82-C91, (2022).
[8] B. Li, *et al.*, OFC 2022, 1-3, paper M3G.1.